Sub-wavelength confinement of the orbital angular momentum of light probed by plasmonic nanorods resonances

Marta Carli,[1,*] Pierfrancesco Zilio,[1] Denis Garoli,[1] Valentina Giorgis,[2] and Filippo Romanato[1,2]

[1]*Department of Physics and Astronomy, University of Padova, Via Marzolo 8, 35131 Padova, Italy*
[2]*CNR-IOM, SS. 14 Km 163.5, Area Science Park, Basovizza, Trieste, Italy*
[*]*marta.carli.1@unipd.it*

Abstract: We discuss how the topological charge of an OAM-carrying plasmon (Plasmonic Vortex) can be probed by monitoring the near-field response of plasmonic nanostructures suitably arranged inside a Plasmonic Vortex Lens. The turning "on" or "off" of four gold nanorods, detected by a Scanning Near field Optical Microscope (SNOM), acts as a fingerprint of the OAM state of the PV at the nanoscale. Different configurations are studied numerically, the integrated structure is fabricated and near field characterization is performed for a particularly meaningful case.

OCIS codes: (050.4865) Optical vortices; (230.0230) Optical devices; (240.6680) Surface plasmons; (160.4236) Nanomaterials.

References and links

1. L. Allen, M. W. Beijersbergen, R. J. Spreeuw, and J. P. Woerdman, "Orbital angular momentum of light and the transformation of Laguerre-Gaussian laser modes," Phys. Rev. A **45**(11), 8185–8189 (1992).
2. Y. Gorodetski, A. Niv, V. Kleiner, and E. Hasman, "Observation of the spin-based plasmonic effect in nanoscale structures," Phys. Rev. Lett. **101**(4), 043903 (2008).
3. S. Yang, W. Chen, R. L. Nelson, and Q. Zhan, "Miniature circular polarization analyzer with spiral plasmonic lens," Opt. Lett. **34**(20), 3047–3049 (2009).
4. K. Y. Bliokh, Y. Gorodetski, V. Kleiner, and E. Hasman, "Coriolis effect in optics: Unified geometric phase and spin-hall effect," Phys. Rev. Lett. **101**(3), 030404 (2008).
5. H. Kim, J. Park, S.-W. Cho, S.-Y. Lee, M. Kang, and B. Lee, "Synthesis and dynamic switching of surface plasmon vortices with plasmonic vortex lens," Nano Lett. **10**(2), 529–536 (2010).
6. S.-W. Cho, J. Park, S.-Y. Lee, H. Kim, and B. Lee, "Coupling of spin and angular momentum of light in plasmonic vortex," Opt. Express **20**(9), 10083–10094 (2012).
7. Y. Gorodetski, N. Shitrit, I. Bretner, V. Kleiner, and E. Hasman, "Observation of optical spin symmetry breaking in nanoapertures," Nano Lett. **9**(8), 3016–3019 (2009).
8. L. T. Vuong, A. J. L. Adam, J. M. Brok, P. C. M. Planken, and H. P. Urbach, "Electromagnetic spin-orbit interactions via scattering of subwavelength apertures," Phys. Rev. Lett. **104**(8), 083903 (2010).
9. P. Zilio, E. Mari, G. Parisi, F. Tamburini, and F. Romanato, "Angular momentum properties of electromagnetic field transmitted through holey plasmonic vortex lenses," Opt. Lett. **37**(15), 3234–3236 (2012).
10. S. A. Maier, *Plasmonics: Fundamentals and Applications* (Springer, 2007).
11. P. Bharadwaj, B. Deutsch, and L. Novotny, "Optical antennae," Adv. Opt. Photon. **1**(3), 438–483 (2009).
12. E. J. Smythe, E. Cubukcu, and F. Capasso, "Optical properties of surface plasmon resonances of coupled metallic nanorods," Opt. Express **15**(12), 7439–7447 (2007).
13. J. Aizpurua, G. W. Bryant, L. J. Richter, F. J. García de Abajo, B. K. Kelley, and T. Mallouk, "Optical properties of coupled metallic nanorods for field-enhanced spectroscopy," Phys. Rev. B **71**(23), 235420 (2005).
14. J. Beermann, S. M. Novikov, K. Leosson, and S. I. Bozhevolnyi, "Surface enhanced Raman imaging: periodic arrays and individual metal nanoparticles," Opt. Express **17**(15), 12698–12705 (2009).
15. P. Genevet, N. Yu, F. Aieta, J. Lin, M. A. Kats, R. Blanchard, M. O. Scully, Z. Gaburro, and F. Capasso, "Ultra-thin plasmonic optical vortex plate based on phase discontinuities," Appl. Phys. Lett. **100**(1), 013101 (2012).
16. F. Aieta, P. Genevet, M. A. Kats, N. Yu, R. Blanchard, Z. Gaburro, and F. Capasso, "Aberration-free ultrathin flat lenses and axicons at telecom wavelengths based on plasmonic metasurfaces," Nano Lett. **12**(9), 4932–4936 (2012).
17. N. Yu, F. Aieta, P. Genevet, M. A. Kats, Z. Gaburro, and F. Capasso, "A broadband, background-free quarter-wave plate based on plasmonic metasurfaces," Nano Lett. **12**(12), 6328–6333 (2012).

#219968 - $15.00 USD Received 28 Jul 2014; revised 14 Sep 2014; accepted 15 Sep 2014; published 17 Oct 2014

18. S. Pancharatnam, "Generalized theory of interference, and its applications," Proc. Indiana Acad. Sci. **A44**, 247 (1956).
19. M. V. Berry, "Quantum phase factors accompanying adiabatic changes," Proc. R. Soc. London A **392**(1802), 45–57 (1984).

1. Introduction

In 1992, in a famous paper, Allen et al. [1] were the first to recognize that light beams with an azimuthal phase dependence $e^{ij\phi}$, j being an integer called the "topological charge", carry an angular momentum, given by the sum of a Spin Angular Momentum (SAM) and of an Orbital Angular Momentum (OAM). Of course, the OAM of light has a history prior to 1992, concerning for instance high-order atomic transitions. The key point of Allen was that this OAM was a natural property of all helical-phased beams, and hence could be readily generated in a standard optics lab. These beams can be described in terms of solutions of the paraxial wave equation in cylindrical coordinates, which are known as Laguerre-Gauss (LG) modes.

In recent years, with the extraordinary development of nanofabrication tools, the question whether plasmonic waves could carry orbital angular momentum like their 3D counterparts has arisen, since this would carry along the possibility of gaining control of OAM of electromagnetic fields and engineering spin-orbit interactions at the nanoscale. This fundamental question has found a positive answer: it has been shown that Surface Plasmon Polaritons (SPPs) can indeed carry OAM and these OAM-carrying 2D waves were termed Plasmonic Vortices (PVs) [2]. PVs can be generated by exploiting particular metallic nanostructures illuminated by circularly polarized light, which convert the SAM of the incident light into OAM taking advantage of plasmonic effects. An outstanding example of such a structure is the Plasmonic Vortex Lens (PVL) [3–7], consisting in Archimedean spiral-shaped grooves milled in a metallic slab. Not only these structures convert the SAM of incident light into PVs, but they also focus the generated PVs to their center, hence the term "lens". As it will be specified in the following sections of this paper, it is possible to control the total topological charge of the generated PV by acting on the polarization of the incident light and on the number of arms of the spiral.

Even more interesting properties arise if a hole is milled at the center of the PVL, as was reported by some groups [7, 8] and recently thoroughly investigated by our group [9], who discussed the characteristics of the focused field inside the hole and beyond it.

In this work, we exploit gold nanorods to probe the local field configuration inside the hole in the near field. We refer as "nanorods" to elongated sub-wavelength metallic structures that support the Localized Surface Plasmon Resonance (LSPR) [10]. More specifically, these structures can be described as ellipse-shaped disks lying on the substrate. An in-plane electric field component can excite two distinct LSPR resonances, one for each of the two axes of the ellipse, with the one along the major axis being red-shifted with respect to the other one [10–12]. The resonance wavelengths depend on the nanorod geometry (length, width, thickness). Structures like these have been studied for different applications, such as spectroscopy [13, 14] or, more recently, for the generation of plasmonic metasurface-based optical elements [15–17].

Our claim is that four nanorods can be used as probes of the OAM of the PV focused by a PVL, provided they are suitably arranged inside a hole milled at the center of the spiral. As hinted above, the excitation of these structures depends on the orientation of the local electric field. This selectivity in direction can be translated into a selectivity in j, due to the close link between the topological charge of the PV and the direction of the field lines inside the hole.

2. Plasmonic vortex generation

Our PVLs consist of an Archimedean spiral-shaped slit milled in a gold film on a glass substrate (Fig. 1). The geometry of the groove is defined by

#219968 - $15.00 USD Received 28 Jul 2014; revised 14 Sep 2014; accepted 15 Sep 2014; published 17 Oct 2014

$$r_m(\varphi) = r_0 + m\frac{d}{2\pi}\varphi \tag{1}$$

being φ the azimuthal angle, d the PVL pitch, m an integer and r_0 the distance from the center to the nearest point of the groove. The complete PVL consists of m spirals, each one rotated of 360/m degrees with respect to the adjacent ones.

The mechanism of PV generation and focusing was described in detail by Gorodetski [2]. A 780 nm circularly polarized plane wave impinges normally from the glass side onto the patterned metal layer. The spiral grating pitch is tuned to enable optimal coupling of light at this wavelength to the SPP mode at the metal-air interface. A SPP in the form of a plasmonic vortex is thus produced thanks to the spiral shape of the slits.

In the case of the *bull's eye* ($m = 0$), an azimuthal phase factor arises due to a polarization-dependent coupling. The origin of this phase factor is purely geometric and it is commonly referred to as Pancharatnam-Berry phase [18, 19]. In spiral structures, an additional phase factor arises as a result of a space-variant path difference and allows to impress an arbitrary topological charge to the resulting PV [5].

The details of the SPP field pattern produced by the PVL are difficult to calculate analytically. However, it has been demonstrated [3] that a good approximation of the field at the PVL center in case of large r_0, neglecting metal losses, is given by

$$E_{SPP,m}(R,\varphi) \propto e^{ij\varphi} J_i(k_{SPP}R) \tag{2}$$

where J_j is the j-th order Bessel function and j is the total topological charge of the focused PV, given by the selection rule [5, 6]

$$j = l + s + m \tag{3}$$

where l is the topological charge of impinging light (assumed to impinge coaxially with the PVL symmetry axis) and s is the SAM quantum number. We notice that formula (2) represents the interference pattern of two PVs, one converging towards the PVL center and one propagating radially in the opposite direction.

In the standard case $l = 0$ and circularly polarized light, Eq. (3) reduces to $j = m \pm 1$. Since the intensity of the field is described by a Bessel function, we expect an intensity pattern with bright and dark concentric rings. In particular, for $j = 0$ a bright spot is expected at the center of the structure, while, for $j>0$, there will be a dark spot at the center and the intensity maximum will be on a ring, the radius of which increases with j.

Knowing the analytical description of the field produced by a PVL enables to numerically study its interaction with nanostructures at its center in an easy way. In fact, most of the FEM scattering simulations presented in the following discussion consider only a small region of the PVL near its center as a simulation domain, as shown in Fig. 1, setting the analytical plasmonic vortex expression in Eq. (2) as a background field. Perfectly Matched Layers (PMLs) are placed all around the physical domain to absorb scattered radiation. In this way, we are able to isolate the optical response of the nanorods resulting from their interaction with the PV from the one related to the interaction with light directly impinging on the PVL center.

#219968 - $15.00 USD Received 28 Jul 2014; revised 14 Sep 2014; accepted 15 Sep 2014; published 17 Oct 2014

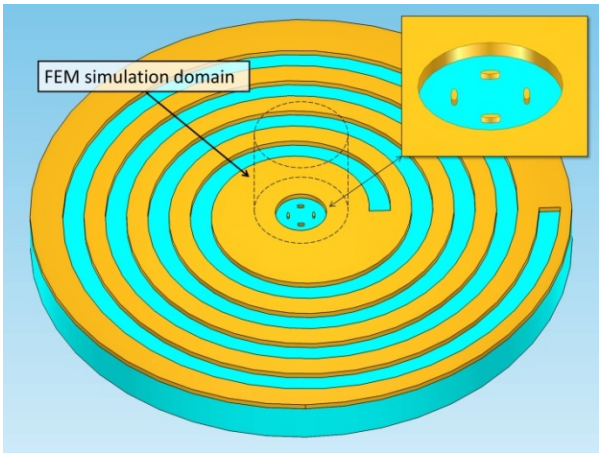

Fig. 1. Geometry of our structure, consisting in a Plasmonic Vortex Lens with $m = 1$, with four nanorods placed in a hole at the center of the spiral (see inset). The dashed cylinder highlights the FEM simulation domain, where the analytical plasmonic vortex expression was set as the background field.

3. Interaction of the PV with gold nanorods

In a recent work by our group [9] we discussed the characteristics of the field inside, and transmitted through, a hole milled at the center of a PVL. In particular, we showed that in-plane components of the electric field are dominant inside the hole for sufficiently large values of its radius. Therefore, one or more nanorods inside the hole can in principle be excited by these components, provided they are arranged in such a way that the field lines are aligned with one of the two axes and their geometry is optimized accordingly. Vice versa, if the arrangement of optimized nanorods is fixed, whether they are turned "on" or "off" depends on the direction of the field lines of the PV which in turns depends on its topological charge.

Let us discuss the conditions under which this matching is possible. As mentioned above, the hole dimensions play an important role in obtaining a relevant plasmonic field inside the hole. If its diameter is large enough, the scattering of the PV at the hole edges allows to efficiently couple one or more localized modes, that can be constructed on the basis of the modes of a cylindrical waveguide.

We performed a study of PV transmission through the hole as a function of the hole radius for different values of j. We considered a 200 nm-thick gold PVL on a glass substrate, assuming a PV incoming to the hole with $\lambda = 780$ nm vacuum wavelength. The results are reported in Fig. 2, where the cases $j = 0,1,2,3$ are shown. Not only the transmission efficiency has maxima for well-defined values of the hole radius, but these optimal radii are also dependent on j. For a given value of j, the maxima correspond to the cut-offs of the modes of the cylindrical waveguide, for increasing radial index. We define the cut-off radius at $\lambda = 780$ nm for a given value of j as the minimum hole radius required to let a relevant fraction of the plasmonic wave impinging onto the hole to be transmitted.

#219968 - $15.00 USD Received 28 Jul 2014; revised 14 Sep 2014; accepted 15 Sep 2014; published 17 Oct 2014

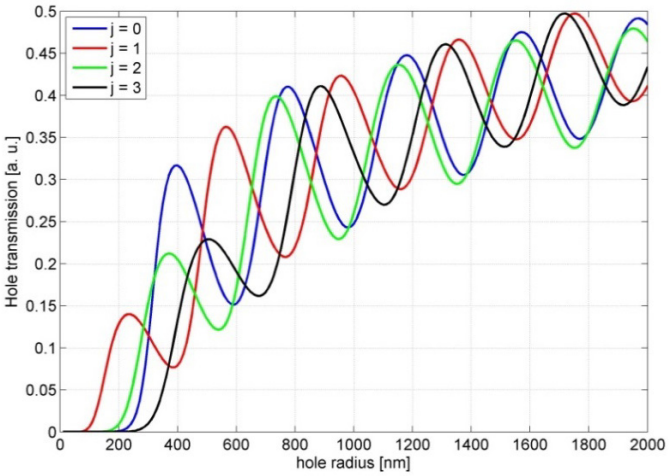

Fig. 2. Power flow as a function of the hole radius for different values of j at λ = 780 nm. For each value of the topological charge we can identify optimal values for the hole radius.

In this study, we considered an m = 1 PVL. According to Eq. (3), such a structure produces PVs with j = 0 or j = 2, depending on the handedness of the circularly-polarized impinging light. As is seen from Fig. 2, a hole radius of 400 nm guarantees a high transmittance for both PVs. To verify how the nanorods influence the transmission properties of the hole, we calculated the transmission spectrum of a hole with r = 400 nm either with or without nanorods at its center. The hole was illuminated by a circularly polarized plane wave, with λ ranging from 650 nm to 950 nm. The plot reported in Fig. 3 suggests that the presence of the nanorods does not dramatically modify the transmission properties of the hole, even if a difference between the cases with and without rods can be observed around the design wavelength λ = 780 nm. The field distributions corresponding to the different cases are reported in the insets.

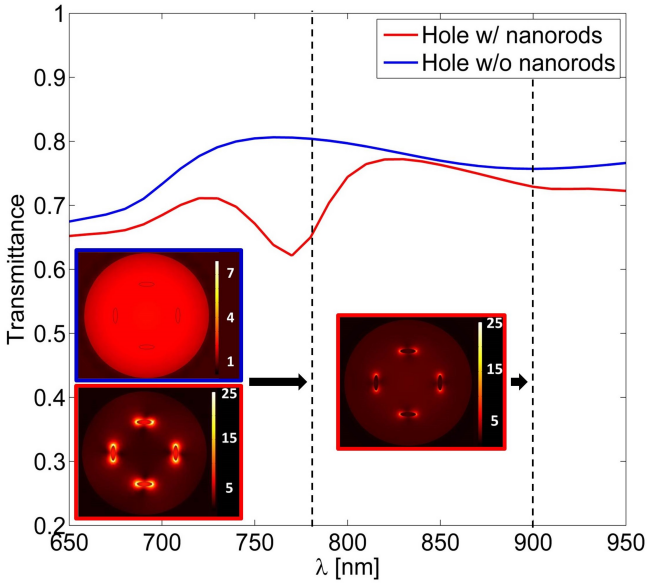

Fig. 3. Calculated transmittance of an 800 nm wide hole on 200 nm thick gold film illuminated by a circularly polarized plane wave, without (blue) or with (red) four nanorods inside. Insets: Electric field norm distribution on the empty hole at 780 nm (blue frame) or on the hole with embedded nanorods at 780 nm or 1000 nm (red frame).

#219968 - $15.00 USD Received 28 Jul 2014; revised 14 Sep 2014; accepted 15 Sep 2014; published 17 Oct 2014

Using r = 400 nm as the hole radius, we simulated a PV with either j = 0 or j = 2 impinging on the simulation domain described above and we calculated the electric field norm on two cross sections. The length (l), width (w) and thickness (t) of the nanorods were optimized numerically, in order to excite the fundamental dipolar resonance along their major axis at λ = 780 nm; the optimal values were l = 110 nm, w = 30 nm and t = 30 nm.

We report the results in Figs. 4(a) and 4(c) for j = 0 and in Fig. 4(b) and Fig. 4(d) for j = 2. Figures 4(a) and 4(b) show the *xz*-cross section of the simulation domain, while Figs. 4(c) and 4(d) show *xy*-cross sections of the hole at z corresponding to the upper rod surfaces, superimposed to arrows indicating the direction of the electric field at a sample time instant in absence of the nanorods. This allows us to relate the excitation of the nanorods with the shape of the field lines.

The plots show that the near field configuration is very different in the two cases. For j = 0, the field lines are radial and thus aligned with the short axis of the rods rather than with the long one; the rods are not optimized for excitation along that axis, and light simply concentrates at the center of the hole. For j = 2 instead, a rotating quadrupole is induced at the hole edge [9]; the direction of the field lines matches that of the long axis of the optimized nanorods, which are excited consequently.

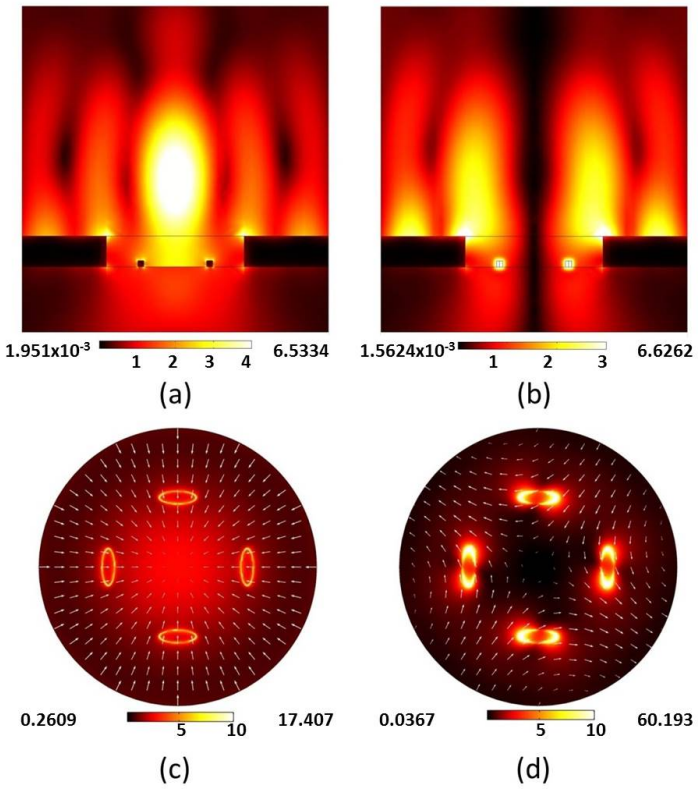

Fig. 4. Electric field norm inside the FEM simulation domain, consisting in a hole at the center of a PVL where four nanorods have been placed. (a) and (b) are *xz*-cross sections of the structure, while (c) and (d) are *xy*-cross sections of the hole; the arrows indicate the direction of the electric field in absence of the rods. The simulations refer to the two cases j = 0 (shown in (a) and (c)) and j = 2 (shown in (b) and (d)). For a better visualization the color scales were saturated to proper values. The minima and maxima of the field for the different plots are reported respectively at the left and at the right of the color bars.

#219968 - $15.00 USD Received 28 Jul 2014; revised 14 Sep 2014; accepted 15 Sep 2014; published 17 Oct 2014

These results suggest a relatively simple way to probe the topological charge of the focused PV, i.e., monitoring the near field of the integrated structure. We expect this kind of measurement to give an easy-to-interpret "on-off" response, due to the strong anisotropy of the nanorods probes configuration discussed above.

4. Fabrication

The structure was fabricated by Electron Beam Lithography (EBL) and electrolytic growth, using a JEOL 6300-FS EBL system operating at 100 keV. The PVL was designed for working in transmission. This means that in Fig. 1 light impinges onto the PVL from the glass side. In literature, PVLs are mostly designed in reflection configuration, with the milled spiral being a groove in the gold slab rather than reaching the dielectric substrate. The SPP coupling efficiency is actually higher in that case. However, since the physics of the device does not change, we chose the transmission configuration since it better suits our experimental setup and enables easy near field measurements. The geometrical parameters of the PVL were optimized by numerical simulations, obtaining d = 758 nm and groove thickness T = 100 nm.

Our substrate was an ITO-coated glass slide (Sigma-Aldrich, thickness 15-30 nm, resistivity 70-100 Ω/cm). We performed an overlay exposure in high resolution; such a process is needed because the sample consists in fact of two layers – the PVL and the nanorods – having different optimal thickness. Two separate metal deposition steps are therefore required. Since the two layers must be precisely aligned to place the rods inside the hole, an alignment process was implemented, which uses lithographed marks placed at a known distance from the structures. A sketch of the fabrication process is reported in Fig. 5.

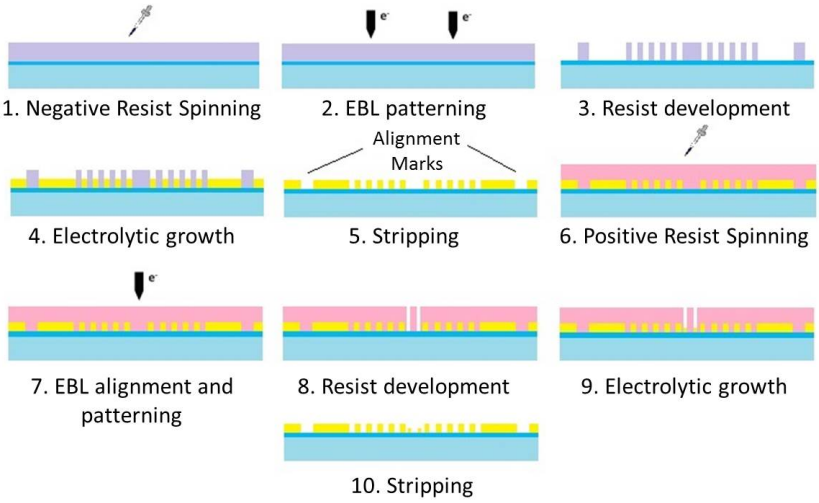

Fig. 5. Scheme of the fabrication process. An EBL overlay exposure was needed. The first layer – consisting in the PVL and the marks used for alignment – was fabricated by EBL on a negative resist, followed by electrolytic growth. The sample was then realigned and the second layer – nanorods inside the hole – was fabricated.

We started by fabricating the first layer, consisting in an array of holey m = 1 PVLs together with global and local marks, needed for the second lithography step; global marks are cross-shaped marks symmetrically placed around the entire exposed area, while local marks are L-shaped marks used for alignment of the single structures. We spin-coated the substrate with negative tone resist (AR-N 7520.073) for 60 s at 4000 rpm obtaining a 400 nm-thick layer; the coated substrate was then baked for 1 minute on a hot plate at 85°C. We patterned the resist with EBL in high resolution, using a beam current of 100 pA and a base dose of 415 μC/cm^2, adjusted point by point using our Genisys^{TM} software, in order to correct

#219968 - $15.00 USD Received 28 Jul 2014; revised 14 Sep 2014; accepted 15 Sep 2014; published 17 Oct 2014

for the proximity effect. The exposed resist was developed in a mixture of the standard negative resist developer AR 300-47 and deionized water (DI H_2O) in a ratio of 4:1 for 150 s. A 100 nm-thick gold layer was deposited by electrolytic growth. The electrolytic bath used in the process is the commercial solution Karatclad 265 HS, with 4.5 nominal pH. The deposition temperature was 34°C, Au 8 g/l, density 15 Bè. A growth current of 100 mA, voltage of 2.9 V and growth time of 50 s was used for the first layer deposition process. Prior to electrochemical growth, the negative resist residuals were removed from the sample surface by Reactive Ion Etching (RIE) in oxygen. Finally, unexposed resist was removed by dipping the substrate in the commercial remover AR 300-70.

To expose the second layer, we deposited 90 nm of commercial positive tone resist (PMMA, AR-P 671.02) onto the surface by spin coating (4000 rpm, 60 s) and soft-baking (180° for 10 minutes). We aligned the system using the marks: their absolute and relative position is detected by the EBL calibration system, which calculates gain and rotation correction parameters. After the second exposure, the resist was developed in a mixture of DI H2O:IPA 3:7 for 30 s (rinse in DI H_2O) and a second electrolytic growth step was carried out. This second layer was grown in the same conditions of the first one for 15 s, obtaining 30 nm-tall nanorods. Unexposed resist was removed by dipping the sample in hot acetone (52° C) for 3 minutes. Some examples of the fabricated structures are shown in Fig. 6.

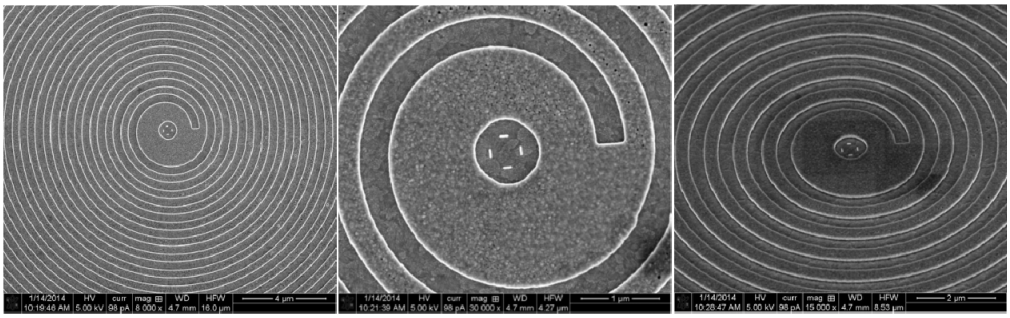

Fig. 6. SEM micrographs of a fabricated sample. (a) The sample consists in an $m = 1$ PVL with four nanorods placed inside the central hole. (b) Zoom in the central part of the device, highlighting the almost perfect alignment of the two exposures. (c) Tilted view highlighting the different thickness of the spiral and of the nanorods.

5. Characterization

As mentioned above, the configuration of the near field of our device is the observable of choice in order to characterize its j-selective behavior. We imaged the near field of our structure using SNOM (Witec Alpha300 S). The sample was illuminated with laser light (λ = 780 nm) from the glass side; the light path comprises a linear polarizer and a quarter wave plate (QWP) to impress the desired circular polarization to the beam before it reaches the sample. With this illumination setup, the $m = 1$ PVL produces PVs with topological charge either $j = 0$ or $j = 2$; switching between the two configurations can be achieved simply by rotating the QWP, which corresponds to modifying s and hence j, according to the selection rule.

The near field signal from the PVL surface is collected in transmission by scanning the sample with a hollow pyramidal probe mounted on a cantilever, and is finally recorded by a photomultiplier. A drawback of this setup is that we expect a non-zero contribution from light directly impinging on the hole. Since we considered multiple turns PVLs, however, the contribution of the plasmonic vortex is expected to be much higher than that of direct illumination.

Results of the near field measurements are presented in Fig. 7, where the two cases of left- and right- circularly polarized illumination ($s = \pm 1$, corresponding to $j = 2$ and $j = 0$,

#219968 - $15.00 USD Received 28 Jul 2014; revised 14 Sep 2014; accepted 15 Sep 2014; published 17 Oct 2014

respectively) are compared. These configurations correspond to the simulations discussed above, where we expect the four rods to be either on or off depending on the topological charge of the generated PV.

The SNOM intensity map for left circular polarization is reported in Fig. 7(a). In this case a $j = 0$ PV is produced by the PVL, and its intensity pattern is characterized by a central spot. Such a PV field is not expected to excite our nanorods. This is actually observed in the experiment: we see an intensity maximum at the PVL center, where light is focused, but no sign of the presence of the rods is seen.

On the other hand, a PV with $j = 2$ is produced by for the opposite circular polarization; it is characterized by a doughnut-shaped intensity pattern. The measured near field map is reported in Fig. 7(b). A bright doughnut is visible, the intensity of which is modulated by the presence of the rods. This modulation is highlighted by the plot in the inset, where the collected light intensity is plotted as a function of a coordinate along the circle of radius 200 nm where the nanorods are located. The four intensity maxima correspond to the four nanorods contribution.

The observed patterns are in good agreement with the discussion and simulated plots reported in Figs. 4(c) and 4(d). As mentioned above, we notice that the center is not completely dark, due to the fact that some light is impinging directly on the hole, and is therefore superimposed to the focused PV. However, the two situations show clearly distinguishable intensity patterns, which proves our assumption that the contribution of direct light is basically a background over which the much more intense focused light is visible.

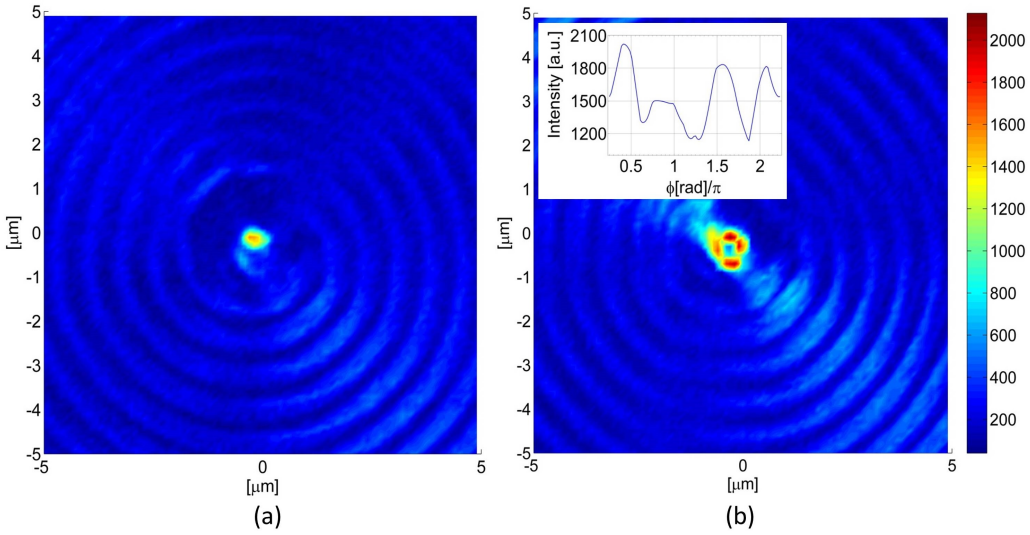

Fig. 7. SNOM scans obtained upon illumination with (a) Case $j = 0$: light is focused to the center but the rods are not excited. (b) Case $j = 2$: all the four rods are illuminated. Inset: plot of light intensity as a function of the azimuthal angle, taken at a fixed radius of 200 nm, corresponding to the position of the rods. The observed modulation highlights the presence of the rods.

6. Conclusions

In this paper, we discussed a way to probe the OAM of light on a sub-wavelength scale. Our approach exploits the localized plasmonic resonances of gold nanorods. Provided the geometry of these structures is properly tuned and they are suitably arranged inside a holey Plasmonic Vortex Lens, they are *j*-selectively turned on and off.

In particular, we studied the near-field properties of the coupled (PVL + nanorod) structure in two cases, $j = 0$ and $j = 2$, that can be obtained by illuminating an $m = 1$ PVL with

#219968 - $15.00 USD Received 28 Jul 2014; revised 14 Sep 2014; accepted 15 Sep 2014; published 17 Oct 2014

either left- or right-handed circularly polarized light. We used four tangentially-arranged gold nanorods as the probes, and their near-field was characterized by SNOM. Our results seem to prove the capability of PVLs to transfer OAM properties control to the nanoscale as well as engineering spin-orbit interactions in the sub-wavelength regime.

It is worth to point out that in this work we only considered the near-field properties of the coupled structure, without investigating the far-field consequences of the coupling. As a matter of fact, near-field measurements provide a clear "on-off" result and are therefore well-suited to experimentally prove the OAM of light inside the hole, while the response in the far-field regime is expected to be less straightforward. However, the analysis of far-field aspects would be an interesting extension to our study, and could be the subject of further investigations.

Acknowledgments

This work was supported by the FONDAZIONE CARIPLO project "Surface-enhanced Coherent Antistokes Raman Scattering for label-free ultra-sensitive detection" (Ref. 2012-0904). The authors also acknowledge Dr. Michele Massari for fruitful discussion about nanofabrication.

#219968 - $15.00 USD Received 28 Jul 2014; revised 14 Sep 2014; accepted 15 Sep 2014; published 17 Oct 2014